Integrated Flood Modeling for Klang River Basin Using HEC-HMS and Radar Rainfall Input

O. N. Shazwani[1], T. Wardah[1,*], C. K. Nursalleh[2]

[1] School of Civil Engineering, College of Engineering, Universiti Teknologi MARA, Shah Alam, Selangor, Malaysia
[2] Malaysian Meteorological Department, Petaling Jaya, Selangor, Malaysia
Email: 2021419378@student.uitm.edu.my (O.N.S.); warda053@uitm.edu.my (T.W.); nursalleh@met.gov.my (C.K.N.)
*Corresponding author

Manuscript received October 26, 2023; revised November 29, 2023; accepted December 12, 2023, published July 17, 2024

***Abstract*—Flooding is one of the most frequent natural disasters in Malaysia, causing billions of ringgits in damages and numerous deaths. One of the key strategies to lessen the impact of the disaster is by flood modelling, which is especially beneficial in flood risk management and decision making. This paper focuses on flood modelling and simulation for a river basin using HEC-HMS software with alternative data input from rainfall data produced by weather radar (QPE). Radar QPE has the advantage of providing an areal representation of rainfall, but it is only an indirect measurement of the values. HEC-HMS is an innovative hydrologic modeling software with the advantage of a moderate processing time compared to the more sophisticated hydrodynamic models yet being reasonably accurate. The study methods include the collection and preparation of data required, such as DEM, land use, and soil type for study area of Klang River basin, Malaysia. Initially, the hydrologic model performed a calibration process using the rain gauge data in an effort to generate the best-quality hydrologic simulations. Subsequently, the rainfall inputs from the mean gridded pixel radar QPE values were then used to rerun the models. After model calibration, the result shows that the coefficient of determination, R^2, for the rain gauge input is higher (0.8) compared to the radar QPE input (0.6). It is concluded that to produce more accurate results, it was recommended that radar QPE calibration was necessary to enhance the data.**

***Keywords*—hydrological modeling, HEC-HMS, model, flood hydrograph, radar QPE**

I. Introduction

Flooding is an inherent natural occurrence resulting from a multitude of contributing factors. The extent of the impacted area, the duration of the flood, and the depth of the flood all vary with flooding. Flooding is the result of water overflowing normally dry areas. Floods can be caused by a number of circumstances, including unusually high and persistent rainfall, growing urbanization, sedimentation from rivers, deforestation, and inadequate drainage systems [1, 2]. Thus, it is crucial to analyze flood events in order to comprehend how the watershed reacts to high rainfall and changes in land use. An accurate peak runoff estimate, obtained from rainfall-runoff simulation, is essential to determining the level of flood risk [3]. Accurate rainfall-runoff modeling is also necessary for the planning and execution of flood control measures in vulnerable areas to reduce the hazards to buildings and the lives of individuals during extreme rainfall events.

A Geographic Information System (GIS) is a computerized system with the capability of collecting, storing, analyzing, and displaying location-based data. This system may be used to model river behavior, forecast floods in real time, and research how river behavior influences floods. It can also be used to predict how a catchment would react to changes in input circumstances [4]. Hydrologic Engineering Corps-Hydrologic Modeling System (HEC-HMS) is a software that simulates precipitation and discharge processes in river basin systems. A number of data sources are utilized, including soil type, Digital Elevation Models (DEMs), and Land Use Land Cover (LULC) for rainfall-runoff modeling [5, 6]. These data can now be easily processed and assessed to determine the parameters of hydrological modeling with the aid of GIS development [7, 8]. The Hydrologic Engineering Center (HEC) created HEC Geo-HMS and an extension tool known as the hydro arc tool in order to construct the HEC-HMS database. In addition, by using DEM, topography analysis is performed utilizing the ArcGIS tool to delineate the watershed and river-stream network. The creation of the fundamental rainfall-runoff model by HEC-HMS requires an understanding of the basin's features, such as reservoir area, slope, river length, etc.

Rain gauges and radars are commonly used to measure and estimate rainfall. Within a specific watershed, the importance of rainfall input in hydrologic models acts as a crucial component for water balance calculations, water distribution forecasts, and flood alerts [9, 10]. The data from rain gauges are commonly assumed to provide accurate estimations at ground interfaces; nevertheless, estimating rainfall spatial variability at any watershed level is difficult [11]. Meanwhile, radar offers real-time, spatial, and temporal data over a large area. The rainfall data produced by weather radar or known as radar Quantitative Precipitation Estimation (QPE) is crucial for hydrological model simulations used in operational flood prediction [12, 13].

Most of the studies by previous researchers made use of extensive rain gauge networks as the time series data input for HEC-HMS model [14]. Rarely are there studies especially in Malaysia, compare the simulated flow output from inputs using both rain gauge and radar data, though several studies on radar QPE had been initiated among others as described in [15, 16]. Additionally, the integration of gridded based radar QPE input with the HEC-HMS model has not been widely studied. This research was planned with these deficiencies in mind, with an emphasis on assessing these variables in hydrologic analysis for Malaysia circumstances. This study aimed to develop an integrated hydro-meteorological flood modeling using HEC-HMS for Klang River basin through the Integration of Digital Elevation Models (DEM), Geographic Information Systems (GIS), and remote sensing with alternative inputs from rain gauge and radar QPE.

This paper will proceed as described below. The literature review is covered in Section II, and the study area and data processing are explained in Section III. The several approaches and combinations used in the HEC-HMS model to replicate rainfall-runoff processes in the Klang River basin are also covered in this section. This section includes a detailed discussion of the parameters and values given in the HEC-HMS model generated during this investigation. Next, the result and discussion are presented in Section IV. Finally, this study concludes with recommendations in Section V.

II. Literature Review

The HEC-HMS is a conceptually driven, deterministic, and semi-distributed hydrological modeling system. Numerous scholars have utilized the HEC-HMS tool in hydrological modeling. This is due to the fact that this application's simulation of direct discharge from precipitation can accurately represent the flow behavior. In Turkey, Barbosa *et al.,* [17] have applied HEC-HMS to computational hydraulic analysis and hydrological process modeling using interface approaches that integrate HEC-HMS and HEC-RAS modeling via GIS, covering the Zab Besar River's floodplains. The results are likewise very good, with a very decent correlation coefficient, after calibration and validation. Martin *et al.,* [18] used hydraulic flow modeling to determine surface runoff using the Arc-Map along with HEC-GeoHMS components. Next, Sapountzis *et al.,* [19] carried out a study to evaluate the application of satellites precipitation data for hydrological studies, including flash flood peak discharge in ungauged Mediterranean basins. On Thasos Island, Greece, linear equations were made based on the relationship between the total height of precipitation from a local rain gauge and the Global Precipitation Measurement and the Integrated Multi-Satellite Retrievals (GPMIMERG) in order to change the uncalibrated GPM-IMERG rainfall data. The hydrological modeling results showed that the uncalibrated GPM-IMERG rainfall data could not predict flash floods. However, rain gauge data input could more accurately simulate peak flow. Additionally, by using extrapolation from linear regression models, it was proposed that the correlation between satellite spatiotemporal precipitation data and ground rainfall data can enhance the effectiveness and precision of flash flood analyses for flood mitigation strategies in ungauged watersheds ($R^2 > 0.65$).

Moreover, HEC-HMS has been used to model rainfall and runoff in a number of Indonesian watersheds. Affandi *et al.,* [20] reported the lowest RMSE value of 3.7, and the Nash approach produced the lowest value of –0.2 in the Sampean Baru basin on Java Island. The same thing has also been done in the Bantimurung Sub-watershed, South Province, where GIS and HEC-HMS work together to simulate hydrological modeling quite well. This is done using a soil texture map from the Ministry of Agriculture of the Republic of Indonesia, which yields R^2 and NSE values of 0.595 and 0.456, respectively [21]. In China, Oleyiblo *et al.,* [22] conducted research in the Wan'an and Misai basins using the HEC-HMS application to anticipate floods. The application was then calibrated and validated using rainfall data obtained from field measurements, yielding results with a reasonably good correlation value.

In addition, numerous earlier investigations demonstrated the HEC-HMS model's suitability for flood simulation. Harka *et al.,* [23] claimed that the model simulation's outcomes were location-specific in this regard. In their 2019 study, Ademe *et al.,* [24] employed the HEC-HMS model to forecast flooding in the watershed of Ethiopia's Lake Tana basin. According to research, the model can replicate floods. In their evaluation of drainage structure failure across Akaki river crossing, Guduru *et al.,* [25] concluded that HEC-HMS accurately approximated design discharge. An analysis of the Seethawaka River, Sri Lanka, through the lens of an event-based streamflow simulation approach was done by Gunatilakhe *et al.,* [26]. The results show that the model created in this work can satisfactorily simulate peak discharges and time their occurrence based on the results of statistical parameters and graphical observations.

Malaysia is a tropical country with high humidity and copious rainfall, amounting to an average of 2000–4000 mm annually. The yearly average rainfall may surpass the range mentioned above, barring exceptionally extreme rainfall events that frequently cause floods in multiple places during the monsoon seasons [27]. Considering this, establishing a policy to evaluate the flood discharge is imperative. The runoff is critically affected by the measurement of all factors; thus, the best model must be selected with the fewest possible input data requirements, an easy-to-understand structure, and realistic accuracy. Studied by Ramly and Tahir [28] simulate rainfall-runoff model by utilizing the HEC-HMS program together with raingauge and DEM data as basin model input in the upper Klang-Ampang River basin, a region close to Malaysia's capital that is prone to flooding. The result shows a reasonable level of accuracy, as shown by the 0.86 Nash-Sutcliffe coefficient. Moreover, Adnan *et al.,* [29] investigate the comparison of changes in land use in the River Kelantan, Malaysia catchment, variations in rainfall patterns led to larger changes in peak flow and runoff volume, as would be predicted given the intense amount of monsoonal rainfall. The result shows the upstream portion of the watershed experienced an intensification of runoff volume due to changes in land use, specifically an increase in urbanized and agricultural areas. Decision-makers, like land use planners, can employ appropriate policies based on this information, such as limiting the rate of urban expansion, especially along rivers and in floodplain zones.

Furthermore, Sukairi *et al.,* [30] study the performance of HEC-HMS and RRI models using raingauge rainfall estimates at Sungai Lebir basin, Kelantan. The calibration of HEC-HMS model yielded NSE values of -9.806 and 0.858, but the model validation yielded values of 0.817 and 0.821. On the other hand, the calibration findings for the RRI model were –0.312 and 0.587, whereas the validation results were 0.786 and 0.731. Throughout the entire time period, the HEC-HMS model was able to produce stream flow values that were more precise than those of the RRI model. After completing the optimization procedure, more accurate results were obtained, and the resulting NSE value increased to 0.611 and 0.467. Both model's overall performance is thought to be satisfactory. The results show that the HEC-HMS software's computed flow rate does not deviate greatly from the actual rate, and they also show that the software is appropriate for application in flow rate estimates.

On top of that, the most popular Soil Water Assessment Tool (ArcSWAT) and HEC-HMS model were compared in order to evaluate the effects of climate change on streamflow in the Bernam basin, Malaysia [31]. The model's performance was adequate. On the other hand, HEC-HMS outperformed ArcSWAT. Several studies have also noted that the HEC-HMS model consistently underestimates peak flows with significantly higher values [32–34]. As a result, the HEC-HMS model needs to be utilized in the research area with extreme caution, particularly when it comes to flood analysis.

III. Materials and Methods

A. Study Area

Klang River basin is the focus of the research. Situated on the western coast of Peninsular Malaysia, the Klang River basin encompasses about a third of Selangor State and has an area of catchment of 1,288.4 km^2. The Klang River basin spans the Federal Territory, including Kuala Lumpur, a significant urban region in Malaysia, as well as the highly developed and industrialized suburbs of Shah Alam, Petaling Jaya, Port Klang and Klang as shown in Fig.1. Recently, this region has experienced rapid expansion and growth. Periodic floods have long been a major barrier to efficient land utilization and high living standards in the region of Klang. Around 14 percent of the administrative area of the Klang Valley (234,347 ha) is susceptible to flooding [27]. The majority of the flooded region is located downstream from the central business district of Kuala Lumpur and close to the Klang River, Selangor.

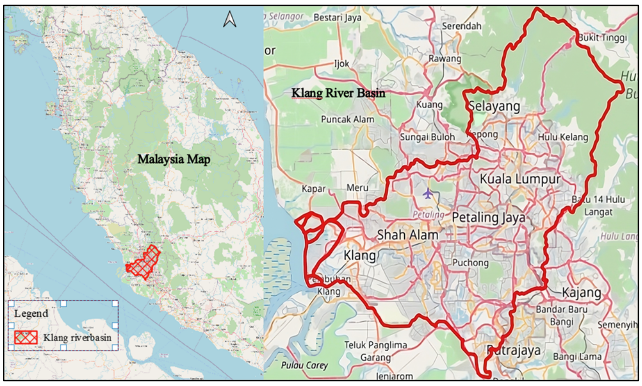

Fig. 1. Location of Klang River basin.

B. Data Processing

This section includes the outline of a systematic approach for the acquisition and organization of data required for the spatial hydrological modeling of the given basin. In this study, the models incorporated both rain gauge rainfall estimation and radar QPE on hourly basis. The weather radar data were retrieved from the Malaysian Meteorological Department (MMD), while rainfall gauge and stream flow data were obtained from the Department of Irrigation and Drainage (DID) in Malaysia. Radar composite products, referred to as Radar Integrated Nowcasting System (RaINS), are produced by mathematically combining data from different radars and radar stations. The products for Peninsular Malaysia are derived by interpolating data from ten radar stations across the Peninsula into a single grid using the inverse distance weighted (IDW) technique. The maximum re-gridded reflectivity data from ten radar stations makes up the final product [35]. The radar reflectivity is converted to rain rate using the Marshall Palmer equation and used as the rainfall input but has not gone calibration process as being done in reference [36]. Fig. 2 displays the radar image corresponding to each subbasin within the Klang River basin. The mean gridded pixel value for each subbasin is computed using the Quantum Geographic Information System (QGIS) software. In addition, for rain gauge data, the areal rainfall for every subbasin over the catchment was computed by averaging the values of all the points known as arithmetic mean analysis method. Next, Arc Hydro and HEC Geo-HMS, which are derivatives of a GIS, were employed in this study in order to prepare the necessary data for this modeling. Additionally, the study entails generating land use and soil maps as well as calculating the curve number grid as shown in the details below. Finally, the basin model is imported into HEC-HMS for further analysis and simulation.

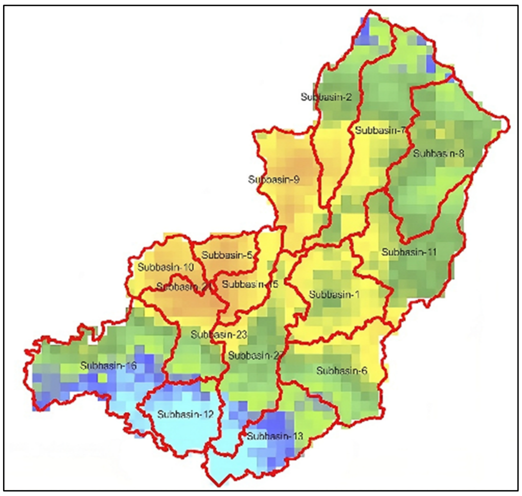

Fig. 2. Uncalibrated radar QPE for the Klang River basin.

1) Digital Elevation Model (DEM)

A topographic map, which is a Digital Elevation Model (DEM) of 30 m or less, as shown in Fig. 3, is required to find the best accuracy on the elevation for every point. It is used to delineate catchments and establish cross-sections of the river. The conventional approach for delineating a watershed area from a topographic map is time-consuming and prone to inaccuracies. Consequently, the basin model is schematized by the automated extraction process facilitated by the DEM and the execution of several operations.

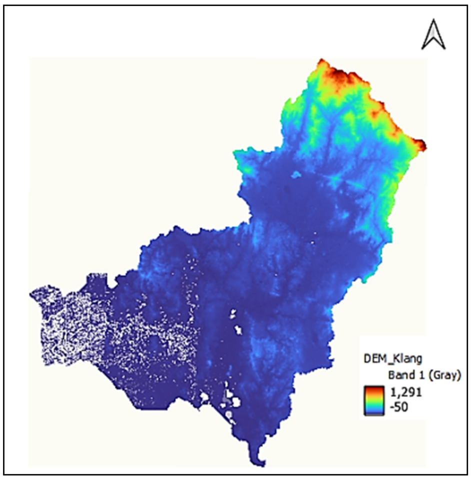

Fig. 3. Digital Elevation Model for the Klang River basin.

2) Soil map

Soil map used to determine the hydrological and further define the CN value of a catchment. It comprises of various types of soil respective to its area covered and can be obtained from Digital Soil Map of the World (DSMW) website. Soil map of the Klang River basin is illustrated as in Fig. 4.

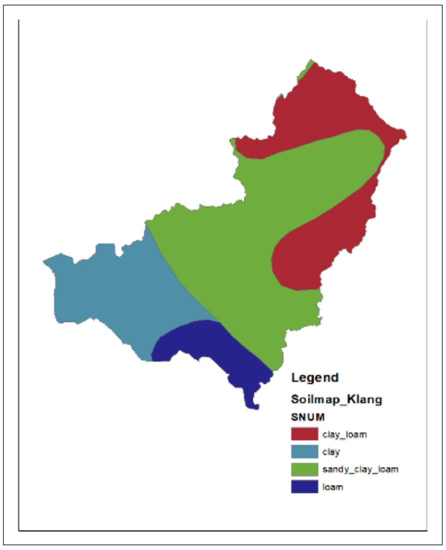

Fig. 4. Hydrologic Soil Group (HSG) for the Klang River basin.

Table 1. Soil texture classes

SNUM	COUNTRY	Texture	Hydrological Group
4284	MALAYSIA	clay-loam	D
4324	MALAYSIA	clay	C
4464	MALAYSIA	sandy-clay-loam	D
4552	MALAYSIA	loam	D

The soil classification used by the Soil Conservation Service (SCS) method is the hydrological classification. It is a classification that consists of grouping soils into four hydrological groups (A, B, C, D), based on their estimated infiltration potential where A represents high infiltration rates in soil, B represents moderate infiltration rates in soil, C represents slow infiltration rates in soil, and D represents extremely slow infiltration rates in soil [37]. The transition from soil classification to hydrological classification is made by providing information on soil texture according to the composition of sandy, clay, and loam, because soil texture information is essential to determine the runoff coefficient [38]. The values of these components are given in the Tables 1 and 2. From this map, it can be concluded that the most dominant class is class D, which shows that the soils have slow infiltration rates and therefore a relatively high runoff.

3) Land use map

Land use map is used to determine the curve number (CN) of a catchment with respect to the soil type of the area. It can be obtained from Land Use and Land Cover (LULC) website. There was data for every country in the world, but only the ones that were connected to the study area were downloaded. Land use data was imported as shape files into ArcGIS until all of the study region was covered. Land use of the Klang catchment is illustrated as in Fig. 5. Table 2 shows the class definition of land use in the Klang watershed referring to ESRI classification [39]. Only the relevant class numbers and class names are listed in the table.

Table 2. Land use classification

Class Number	Class Name
1	water
2	forest
4	mangrove swamp
5	crops
7	built area
8	bare ground
11	rangeland

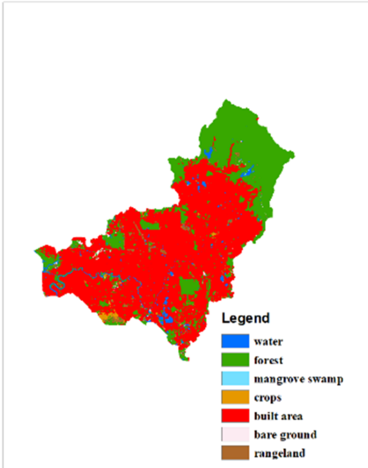

Fig. 5. Land use for the Klang River basin.

4) CN-lookup table

The lookup table shall comprise the CN corresponding to various land use and soil group combinations. The objective of this table is to provide a comprehensive definition of the CN associated with each combination of land use and hydrological group. In this particular scenario, we will employ the SCS curve figures derived from the literature [40]. Table 3 presents a comprehensive summary of the CN-Lookup table, which has been generated based on the land use classes and their corresponding hydrological groups.

Table 3. Initial CN values for land use and hydrological soils group

Land use	HSG			
	A	B	C	D
Water	100	100	100	100
Forest	25	55	70	77
Rangeland	66	77	88	94
Bare ground	72	82	88	90
Built area	77	85	90	92
Mangrove swamp	77	80	83	86
Crops	65	75	82	85

5) CN grid

The HEC-GeoHMS tool within the ArcGIS software platform is utilized for the purpose of generating the CN grid. It incorporates the basin's DEM, the CN-Lookup table, and the union result of soil type and land use. The final CN map of Klang watershed shown in Fig. 6.

The SCS-CN approach was chosen as the loss approach for each of the sub-basins in the Klang watershed. It is employed to calculate the potential runoff following a rainfall event by considering the interplay between soil type, land use, and hydrologic soil conditions. The antecedent moisture condition (AMC) is a hydrologic soil condition that characterizes the soil moisture levels that existed before the simulated rainfall event. AMC I is applied to basins that experienced minimal precipitation prior to the modeled event, while AMC III is utilized in basins that received substantial precipitation prior to the modeled event. AMC II is typically utilized in modeling applications and could be regarded as the average condition. Eqs. (1) and (2) demonstrate how adjustment factors are applied to the CN corresponding to the AMC II condition in order to obtain curve numbers corresponding to AMC conditions I and III [41].

$$AMCI = \frac{4.2 \times AMCII}{10-(0.058 \times AMCII)} \quad (1)$$

$$AMCIII = \frac{23 \times AMCII}{10+(0.13 \times AMCII)} \quad (2)$$

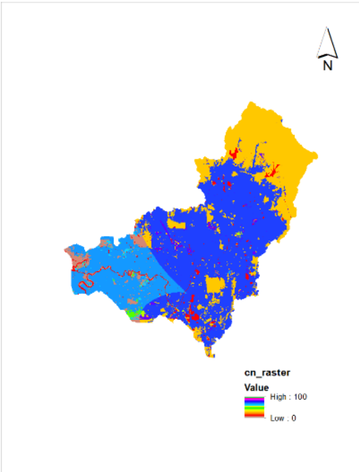

Fig. 6. CN map of Klang River basin.

C. HEC- HMS Model

The HEC-HMS model is widely recognized and extensively utilized throughout various hydrological studies owing to its capacity to accurately simulate runoff for both short and long events, as well as its user-friendly interface [42,43]. There are several model components that are provided, including the basin model, meteorological model, control specification, and time series data input [44]. The input for the meteorological model consisted of rainfall and streamflow data. Furthermore, the control requirements component regulates the duration of the simulation period. The control specifications for the model encompassed the time period from December 18, 2021, to December 22, 2021, with a time step of one hour.

The SCS-CN loss method was used to calculate the initial runoff from a particular or designed rainfall in this study. The accumulated rainfall excess is dependent on soil type, land use, cumulative precipitation, and preceding moisture conditions, as determined in the Eq. (3) [45]:

$$P_e = \frac{(P-I_a)^2}{P-I_a+S} \quad (3)$$

where *Pe*=accumulated precipitation excess at time *t*,
P =accumulated rainfall depth at time *t*,
I_a=the initial abstraction (0.2S),
S =potential maximum retention.

Maximum retention (S) is connected to watershed characteristics (via the dimensionless CN) as Eq. (4):

$$S = 25400 - \frac{254 \times CN}{CN} \quad (4)$$

The SCS-CN is a parameter utilized to depict the cumulative impacts of the primary attributes of the area of catchment. In terms of the transform method, the SCS Unit Hydrograph model was selected to convert excess precipitation into runoff. For this approach, the single input is the lag time (Tlag) which means the time from the excess rainfall center of mass to the hydrograph peak and is determined by concentration time, Tc, as shown in Eq. (5):

$$Tlag = 0.6Tc \quad (5)$$

where the variables *Tlag* and *Tc* represent time intervals measured in minutes.

The Muskingum approach, proposed by McCarthy [31], has been chosen as the routing method. The process enables the determination of the downstream outflow hydrograph of the channel based on the upstream inflow hydrograph. Two parameters are required: the flood wave's travel duration (K) via the routing reach and the dimensionless weight (X), which represents the flood wave's attenuation as it passes through the reach. Typically, measured discharge hydrographs are used to calibrate the models and determine the routing parameters [46].

D. Model Calibration

Both manual and automatic calibration procedures were employed to optimize the parameters of HEC-HMS. Most modeling studies often employ sensitivity analysis to determine the key variables and parameter precision necessary for calibration. The sensitivity factors were chosen based on their impact on the maximum discharge and overall volume. In addition, the calibration of the model was performed using the Peak-Weighted Root Mean Square Error (PWRMS) objective function, as this method was chosen for its simplicity and effectiveness [47]. Possible adjustments to watershed parameters, including curve number, Tlag, baseflow, and initial abstraction may be necessary to achieve an optimal correspondence between simulation results and observations.

Next, the effectiveness of the model and the chosen loss and transform method was assessed by comparing observed streamflow to model-simulated values using statistical evaluation criteria such as coefficient of determination (R^2) (Eq. 6), percent bias (PBIAS) (Eq. 7), Nash–Sutcliffe Efficiency (NSE) (Eq. 8) and Root mean square error-standard deviation ratio (RSR) (Eq. 9).

$$R^2 = \left[\frac{\frac{1}{M}\sum_{k=1}^{M}[(Q_s)_k-\overline{Q_s}][(Q_o)_k-\overline{Q_o}]}{\sqrt{\frac{1}{M}\sum_{k=1}^{M}[(Q_s)_k-\overline{Q_s}]^2}\sqrt{\frac{1}{M}\sum_{k=1}^{M}[(Q_o)_k-\overline{Q_o}]^2}}\right]^2 \quad (6)$$

$$PBIAS = \frac{\sum_{k=1}^{n}[(Q_o)_k-(Q_s)_k]}{\sum_{k=1}^{n}(Q_o)_k} \times 100\% \quad (7)$$

$$NSE = 1 - \frac{\sum_{k=1}^{n}[(Q_o)_k-(Q_s)_k]^2}{\sum_{k=1}^{n}[(Q_o)_k-\overline{Q_o}]^2} \quad (8)$$

$$RSR = \frac{\sqrt{\sum_{k=1}^{n}[(Q_o)_k-(Q_s)_k]^2}}{\sqrt{\sum_{k=1}^{n}[(Q_o)_k-\overline{Q_o}]^2}} \quad (9)$$

where, $(Qo)k$, $(Qs)k$ are the k^{th} observed and simulated discharges respectively; $\overline{Q_o}$ = mean observed discharge; n is the total number of reference data points.

IV. Result and Discussion

A. Watershed Parameters

Table 4 shows the different watershed factors that were used to calibrate the model. For example, there was a spatial variation in the CN value. The weighted curve's overall numbers fall between 80.0 and 91.6. Furthermore, Subbasin-16 has the watershed's highest basin slope, which is 24.9%. On the other hand, Fig. 7 shows results of the sub-basin schematic diagram in HEC-HMS modeling.

B. Model Simulation Result

The findings of hydrological model employed in this study exhibited a satisfactory correlation among the simulated and observed hydrographs subsequent to the optimization process. Table 5 displays the computed percent error in total volume and peak flow between observed and simulated values in raingauge and radar QPE simulations prior to optimization. These values, which are respectively 37.5% and 22.8% for the total volume and 29.6% and 23.7% for the peak flow, indicate that the error was approximately high. This finding led to the sensitivity analysis being carried out to identify the most sensitive parameter. It was discovered that while flood traveling time (k) was more insensitive, Tlag and CN were more sensitive. The range values of each parameter have been adjusted from +10% to -10%, and this adjustment is considered acceptable [48]. As demonstrated in Table 6, following optimization, the RE for raingauge rainfall estimation decreased to 2.1% for the peak flow and 0.1% for the total volume, while the RE for radar QPE decreased to 0.2% for the peak flow and 1.0% for the total volume, respectively. According to Rizal *et al.,* [21] the outcome is quite satisfactory, with acceptable ranges of relative percent errors between observed and simulated values of less than 20%.

Table 4. Watershed parameters generated by HEC-GeoHMS for Klang River basin

Subbasin	Area (KM^2)	Lag Time (min)	Basin Slope (%)	CN
Subbasin-1	77.8	115.0	13.2	91.2
Subbasin-10	34.6	94.7	14.6	88.8
Subbasin-11	97.0	146.6	17.7	87.9
Subbasin-12	51.3	129.2	6.7	90.2
Subbasin-13	70.9	156.0	11.8	88.6
Subbasin-15	35.5	222.7	7.8	90.5
Subbasin-16	127.9	115.5	29.4	88.3
Subbasin-2	72.4	203.2	10.5	81.8
Subbasin-23	60.5	224.0	9.0	90.5
Subbasin-27	103.4	93.7	13.2	91.6
Subbasin-5	25.2	83.6	13.2	87.7
Subbasin-6	82.8	136.4	12.9	90.1
Subbasin-7	124.2	173.5	26.9	82.6
Subbasin-8	116.3	148.1	28.9	80.0
Subbasin-9	67.9	108.9	16.5	87.9

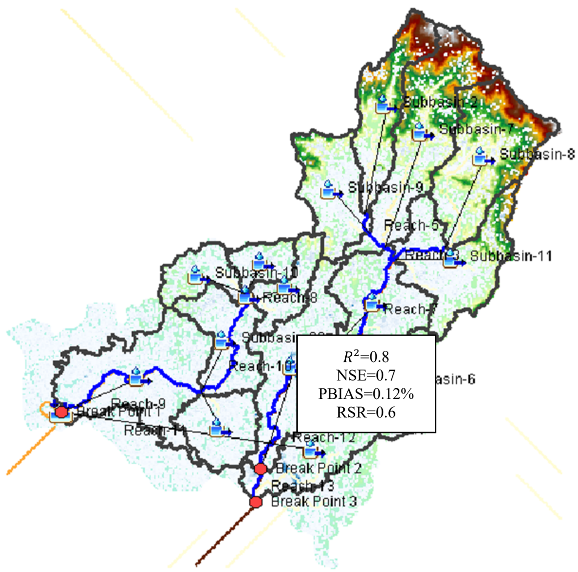

Fig. 7. HEC-HMS sub-basins schematic diagram.

Table 5. Simulated and observed peak discharges and total volume and their evaluation criteria before calibration

	Total volume (mm)			Peak discharge (m^3/s)			R^2	NSE	PBIAS (%)	RSR
	Simulated	Observed	RE	Simulated	Observed	RE				
Rain gauge	130.5	208.9	–37.5	905.2	1286.4	–29.6	0.3	–0.6	–37.5	1.3
Radar QPE	161.3	208.9	–22.8	981.1	1286.4	–23.7	0.2	–0.3	–22.7	1.2

RE: relative error; R^2 : correlation coefficient; NSE: Sutcliffe Efficiency; PBIAS: percent bias; RSR: Root mean square error–standard deviation ratio

Table 6. Simulated and observed peak discharges and total volume and their evaluation criteria after calibration

	Total volume (mm)			Peak discharge (m^3/s)			R^2	NSE	PBIAS (%)	RSR
	Simulated	Observed	RE	Simulated	Observed	RE				
Rain gauge	216.3	216.0	0.1	1313.7	1286.4	2.1	0.8	0.7	0.1	0.6
Radar QPE	218.2	216.0	1.0	1284.2	1286.4	–0.2	0.6	0.5	1.0	0.7

RE: relative error; R^2 : correlation coefficient; NSE: Sutcliffe Efficiency; PBIAS: percent bias; RSR: Root mean square error–standard deviation ratio

The results shown in Table 6 also show a pretty good match between the measured and predicted peak flow rates for raingauge rainfall (R^2= 0.8) during the calibration period compared to radar QPE (R^2= 0.6). The correlation coefficient (>0.8) found in this investigation can be regarded as strong based on the classification described in Zou *et al.,* [49]. Better results were found between the simulated and actual values for the Nash–Sutcliffe Efficiency (NSE) criteria. The model performs satisfactorily, with an NSE value of 0.7 for raingauge estimation and 0.5 for radar QPE. According to Moriasi *et al.,* [50], if the Nash–Sutcliffe efficiency of the model simulation is more than 0.5, it is considered satisfactory; if it is more than 0.65, it is considered good; and if it is more than 0.75, it is considered very good. An NSE value of 1 represents a model that predicts perfectly.

In addition, the simulation performance of raingauge rainfall is somewhat better than radar QPE when measured by the ratio of the standard deviation of observations to the root mean square error (RSR)value. Based on the value of 0.6 acquired, the model can be deemed suitable if RSR is less than 0.7 [51]. Conversely, a model's capacity to replicate a basin's hydrological features increases with decreasing RSR values. As a result, good simulation between the estimated and observed values was demonstrated by rain gauge data, as evidenced by the four statistical assessment criteria with values of NSE = 0.7, R^2 = 0.8, PBIAS = 0.1, and RSR = 0.6.

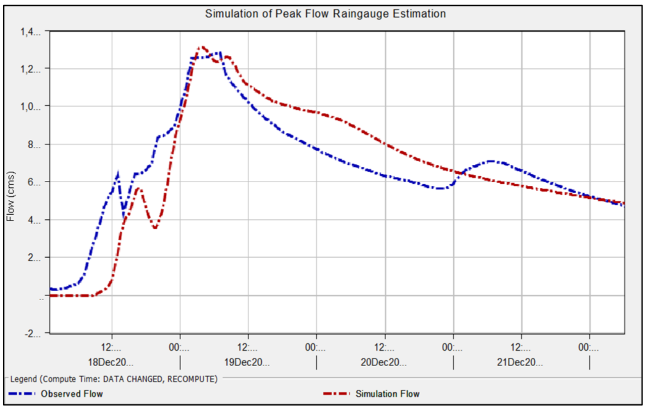

Fig. 8. Simulated and observed hydrograph using raingauge estimate rainfall after calibration.

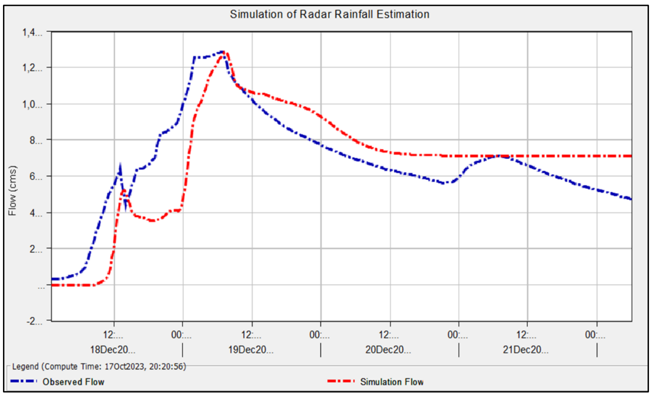

Fig. 9. Simulated and observed hydrograph using radar QPE after calibration.

Figs. 8 and 9 illustrate the comparison hydrograph between the runoff simulations using rain gauge and radar QPE after model calibration. The blue line represents the streamflow data obtained at the Rantau Panjang station, while the red line represents the flow that the model generated. In both rainfall estimation, the hydrograph shape was accurately reproduced in the model output. Specifically, the shape of the hydrograph and its peak time matched well. In Fig. 8, the runoff simulation by raingauge shows the computed volume was 216.3 mm, which is very close to the observed volume (216.0 mm). It can also be seen that the observed peak discharge on December 18, 2021, was about 1286.4 m^3/s and the computed peak discharge was about 1313.7 m^3/s with an accepted percent error of 2.1%. Besides, the computed volume discharged by radar QPE (218.2 mm) shows slightly higher than observed volume (216.0 mm) as shown in Fig. 9. The result shows that the peak discharge that was simulated (1284.2 mm^3/s) on December 18, 2021, was slightly underestimated compared to the observed peak discharge (1286.4 mm^3/s), with a percent error of 0.2%. Both simulated hydrographs show that this HEC–HMS model successfully captures the peak discharge by taking into account the distributed–mode spatial variability of meteorological parameters.

Rain gauges data have the advantage over weather radar QPE because they can precisely measure rainfall at a single spot. Extreme rainfall events surpass the precision of radar QPE. This is due to the large margin of error that results from inferring rainfall intensity from radar reflectivity measurements [52]. It should be highlighted that precisely calculating rainfall using radar remains a challenging issue, even with advancements in radar technology and development. This is mainly due to the fact that indirectly estimating rainfall using radar QPE is limited by locations at heights greater than or equal to the radar station [53]. Furthermore, it is important to have observed rainfall data to establish a comparison with radar QPE as a benchmark before entering the data into the modeling process to assess rainfall or flooding in a particular area. Nevertheless, radar QPE has proven to be a very effective alternative to gauge rainfall and will be of significant use especially for areas with sparsely installed gauges.

V. Conclusion

This study focuses on the methodology for the setup of a rainfall–runoff model using the HEC–HMS software incorporating two different sources of rainfall input. The simulation results from the SCS loss and transform methods were good, and the HEC–HMS model performed satisfactorily in estimating the peak flow and total volume for both rain gauge data and radar QPE input in the watershed of Klang River basin. The statistical analysis demonstrated that when comparing simulated and observed streamflow, the rain gauge data produced more accurate results than the uncalibrated radar QPE. Therefore, radar QPE calibration methods can be performed using radar–gauge merging to ensure the enhancement of simulation results acquired from the radar data. For future work, validation of the model is required in order to ensure that the model parameters function outside of the flow circumstances used for calibration. In addition, since the flow data in this study are insufficient to precisely estimate the flows at the particular outlet, it is advised to set up additional discharge gauge stations in the watershed to improve the model's performance in simulating runoff.

Conflict of Interest

The authors declare no conflict of interest.

Author Contributions

Conducted the research, O.N.S; analyzed data, O.N.S.; writing—original draft preparation, O.N.S.; writing—review and editing, T.W.; data provider and analyzer, C.K.N; all authors had approved the final version.

FUNDING

The authors gratefully acknowledge the Ministry of Higher Education (MOHE) for funding under the Fundamental Research Grant Scheme (FRGS) (FRGS/1/2021/TK0/UiTM/01/1).

ACKNOWLEDGMENT

We would like to express our gratitude towards the Drainage and Irrigation Department and the Malaysian Meteorological Department for providing the data needed for this research.

REFERENCES

[1] L. A. Jabbar, I. A. Khalil, and L. M. Sidek, "HEC–HMS hydrological modelling for runoff estimation in Cameron Highlands, Malaysia," *International Journal of Civil Engineering and Technology*, vol. 12, no. 9, pp. 40–51, 2021.

[2] A. F. M. Mohammed, M. S. Adnan, A. Muneer, S. Sadeq, November, "Flood estimation studies Using Hydrologic Modelling System (HEC–HMS) for Batu Pahat River Malaysia," in *Proc. 2021 Third International Sustainability and Resilience Conference: Climate Change*, IEEE, 2021, pp. 225–230.

[3] L. Schoppa, M. Disse, and S. Bachmair, "Evaluating the performance of random forest for large–scale flood discharge simulation," *Journal of Hydrology*, vol. 590, p. 125531, 2020.

[4] E. Koltsida and A. Kallioras, "Groundwater flow simulation through the application of the FREEWAT modeling platform," *Journal of Hydroinformatics*, vol. 21, no. 5, pp. 812–833, 2019.

[5] A. Banerjee, A. P. Dimri, and K. Kumar, "Rainfall over the Himalayan foot–hill region: Present and future," *Journal of Earth System Science*, vol. 129, no. 11, pp. 1–16, 2020.

[6] D. Kumar and R. K. Bhattacharjya, "Change in rainfall patterns in the hilly region of Uttarakhand due to the impact of climate change," *Applied Environmental Research*, vol. 43, no. 1, pp. 1–13, 2021.

[7] D. Kumar and S. K. Himanshu, "Geographical information based evaluation system for drought," *Water Policy*, vol. 3, no. 4, pp. 49–53, 2017.

[8] C. M. Kazezyilmaz–Alhan, K. Yalcin, K. Javanshour, M. Aytekin, and S. Gulbaz, "A hydrological moel for Ayamama watershed in Istanbul, Turkey, using HEC–HMS," *Water Practice and Technology*, vol. 16, no. 1, pp. 154–161, 2021.

[9] P. Gilewski and M. Nawalany, "Inter–comparison of rain–gauge, radar, and satellite (IMERG GPM) precipitation estimates performance for rainfall–runoff modeling in a mountainous catchment in Poland," *Water*, vol. 10, no. 11, p. 1665, 2018.

[10] T. Nakatani, R. Misumi *et al*., "The role of the spatial distribution of radar rainfall on hydrological modeling for an urbanized river basin in Japan," *Water*, vol. 11, no. 8, p. 1703, 2019.

[11] G. A. P. Eryani, I. M. S. Amerta, and M. W. Jayantari, "Model calibration parameter using optimization trial in HEC–HMS for Unda Watershed," in *Proc. IOP Conference Series: Earth and Environmental Science*, 2021, vol. 930, no. 1, p. 012040, IOP Publishing.

[12] J. P. Looper and B. E. Vieux, "An assessment of distributed flash flood forecasting accuracy using radar and rain gauge input for a physics–based distributed hydrologic model," *Journal of Hydrology*, vol. 412, pp. 114–132, 2012.

[13] P. Rapant and J. Kolejka, "Dynamic pluvial flash flooding hazard forecast using weather radar data," *Remote Sensing*, vol. 13, no. 15, pp. 2943, 2021.

[14] S. Ramly, W. Tahir, J. Jani, S. Sharifi, and J. Abdullah, "Coupling of cellular automata urban growth model and HEC–HMS to predict future flood extents in the upper Klang Ampang catchment," *International Journal of Integrated Engineering*, vol. 14, no. 5, pp. 154–167, 2022.

[15] T. Wardah, R. Suzana, and S. S. N. Huda, "Multi–sensor data inputs rainfall estimation for flood simulation and forecasting," in *Proc.* 2012 *IEEE Colloquium on Humanities, Science and Engineering (CHUSER)*, 2012, pp. 374–379, IEEE.

[16] T. Wardah, S. S. N. Huda, S. M. Deni, and B. N. Azwa, "Radar rainfall estimates comparison with kriging interpolation of gauged rain," in *Proc.* 2*011 IEEE Colloquium on Humanities, Science and Engineering*, 2011, pp. 93–97, IEEE.

[17] J. H. S. Barbosa, A. Fernandes, A. Lima, and L. Assis, "The influence of spatial discretization on HEC–HMS modelling: A case study," *International Journal of Hydrology*, vol. 3, no. 5, pp. 442–449, 2019.

[18] O. Martin, A. Rugumayo, and J. Ovcharovichova, "Application of HEC–HMS/RAS and GIS tools in flood modeling: A case study for river Sironko–Uganda," *Global Journal of Engineering Design and Technology*, vol. 1, no. 2, pp. 19–31, 2012.

[19] M. Sapountzis, A. Kastridis, A. P. Kazamias, A. Karagiannidis, P. Nikopoulos, and K. Lagouvardos, "Utilization and uncertainties of satellite precipitation data in flash flood hydrological analysis in ungauged watersheds," *Glob. Nest J*, vol. *23*, pp. 388–399, 2021.

[20] G. El Afandi, M. Morsy, and F. El Hussieny, "Heavy rainfall simulation over sinai peninsula using the weather research and forecasting model," *International Journal of Atmospheric Sciences*, 2013.

[21] N. S. Rizal, I. Umarie, K. Munandar, and A. E. Wardoyo, "Calibration and validation of CN values for watershed hydrological response," *Civil Engineering Journal*, vol. 9, no. 1, pp. 72–85, 2023.

[22] J. O. Oleyiblo, and Z. J. Li, Application of HEC–HMS for flood forecasting in Misai and Wan'an catchments in China," *Water Science and Engineering*, vol. 3, no. 1, pp. 14–22, 2010.

[23] A. E. Harka, N. B. Jilo, and F. Behulu, "Spatial–temporal rainfall trend and variability assessment in the Upper Wabe Shebelle River Basin, Ethiopia: Application of innovative trend analysis method," *Journal of Hydrology: Regional Studies*, vol. *37*, p. 100915, 2021.

[24] F. Ademe, K. Kibret, S. Beyene, M. Getinet, and G. Mitike, "Rainfall analysis for rain–fed farming in the Great Rift Valley Basins of Ethiopia," *Journal of Water and Climate Change*, vol. 11, no. 3, pp. 812–828, 2020.

[25] J. U. Guduru, N. B. Jilo, Z. A. Rabba, and W. G. Namara, "Rainfall–runoff modeling using HEC–HMS model for Meki River watershed, rift valley basin, Ethiopia," *Journal of African Earth Sciences*, vol. 197, p. 104743, 2023.

[26] M. B. Gunathilake, P. Panditharathne, A. S. Gunathilake, and N. Warakagoda, "Application of a HEC–HMS model on event–based simulations in a tropical watershed," *Engineering and Applied Science Research*, vol. 47, no. 4, pp. 349–360, 2020.

[27] H. K. Loi, "Flood mitigation and flood risk management in Malaysia," in *Proc. International Workshop on Floodplain Risk Management*, 1996, vol. 205, p. 216.

[28] S. Ramly and W. Tahir, "Application of HEC–GeoHMS and HEC–HMS as rainfall–runoff model for flood simulation," in *Proc. the International Symposium on Flood Research and Management*, 2016, pp. 181–192, Springer Singapore.

[29] N. A. Adnan, P. M. Atkinson, Z. M. Yusoff, and A. R. A. Rasam, "Climate variability and anthropogenic impacts on a semi–distributed monsoon catchment runoff simulations," in *Proc. 2014 IEEE 10th International Colloquium on Signal Processing and its Applications*, 2014, pp. 178–183, IEEE.

[30] M. S. Sukairi, S. Harun, K. A. Mohd Nasir, P. Jeevaragagam, and M. R. Mohd Salleh, "Application of geospatial and hydrological modeling for runoff estimation in Lebir River Basin, Malaysia," *The International Archives of the Photogrammetry, Remote Sensing and Spatial Information Sciences*, vol. 48, pp. 231–235, 2023.

[31] H. Ismail, M. R. Kamal, L. S. Hin, and A. F. Abdullah "Performance of HEC–HMS and ArcSWAT Models for assessing climate change impacts on streamflow at Bernam River Basin in Malaysia," *Pertanika Journal of Science and Technology*, vol. *28*, no. 3, 2020.

[32] S. H. M. N. Azam, W. Tahir, and J. Abdullah, "Assessment of SRTM, ASTER and IFSAR digital elevation model (DEM) in oil palm plantation river derivation and basin delineation," in *Proc. the 6th International Conference on Civil, Offshore and Environmental Engineering (ICCOEE2020)*, 2021, pp. 56–65, Springer Singapore.

[33] N. S. Romali, Z. Yusop, and A. Z. Ismail, "Hydrological modelling using HEC–HMS for flood risk assessment of Segamat Town, Malaysia," in *Proc. IOP Conference Series: Materials Science and Engineering*, 2018, vol. 318, no. 1, p. 012029, IOP Publishing.

[34] S. Ramly, W. Tahir, J. Abdullah, J. Jani, S. Ramli, and A. Asmat, "Flood estimation for SMART control operation using integrated radar rainfall input with the HEC–HMS model," *Water Resources Management*, vol. 34, pp. 3113–3127, 2020.

[35] D. J. Yik, Y. W. Sang, N. K. Chang, F. J. Fakaruddin, A. Dindang, and M. H. Abdullah, "Analysis of the cyclonic vortex and evaluation of the performance of the radar integrated nowcasting system (RAINS) during the heavy rainfall episode which caused flooding in Penang, Malaysia on 5 November 2017," *Tropical Cyclone Research and Review*, vol. 7, no. 4, pp. 217–229, 2018.

[36] W. Tahir, M. A. M. Ariffin *et al.*, "Mean field bias correction to radar QPE as input to flood modeling for Malaysian River Basins," *International Journal of Integrated Engineering*, vol. 14, no. 5, pp. 168–177, 2022.

[37] USDA (United States Department of Agriculture), *Urban Hydrology for Small Watersheds, Technical Release 55*, United States Department

of Agriculture, Natural Resources Conservation Services, Conservation Engineering Division, Washington, DC, USA. 2nd ed., 1986.
[38] S. Shadeed and M. Almasri, "Application of GIS–based SCS–CN method in West Bank catchments, Palestine," *Water Science and Engineering*, vol. 3, no. 1, pp. 1–13, 2010.
[39] Sentinel–2 10m land use/land cover time series of the world. Produced by Impact Observatory and Esri. (November 2021). [Online]. Available: https://www.arcgis.com/home/item.html?id=cfcb7609de5f478eb7666240902d4d3d
[40] N. N. Rosli, "Flood modeling and simulation for different landuse pattern using Hec–Hms Model: Case study of the upper catchments of the Kelantan River," BE(Hons)(Civil), Dept. Civil. Eng., Univ. Tech. MARA., Malaysia, 2021.
[41] A. E. Tranceto, "Comparison of hydrologic model performance statistics using thiessen polygon rain gauge and NEXRAD precipitation input methods at different watershed spatial scales and rainfall return frequencies," M.S. thesis, Dept. Civil. Eng., Univ. of. North. Flori., USA, 2015.
[42] B. G. Tassew, M. A. Belete, and K. Miegel, "Application of HEC–HMS model for flow simulation in the Lake Tana basin: The case of Gilgel Abay catchment, upper Blue Nile basin, Ethiopia," *Hydrology*, vol. 6, no. 1, p. 21, 2019.
[43] F. Daide, R. Afgane, A. Lahrach, A. A. Chaouni, M. Msaddek, and I. Elhasnaoui, "Application of the HEC–HMS hydrological model in the Beht watershed (Morocco)," in *Proc. E3S Web of Conferences*, 2021, vol. 314, p. 05003, EDP Sciences.
[44] M. Fleming, "Description of the hydrologic engineering center's hydrologic modeling system (HEC–HMS) and application to watershed studies," ERDC/TN SMART–04–3, 2004.
[45] S. K. Mishra, and V. Singh, *Soil Conservation Service Curve Number (SCS–CN) Methodology*, vol. 42, Springer Science and Business Media, 2003.
[46] A. L. Birkhead and C. S. James, "Muskingum river routing with dynamic bank storage," *Journal of Hydrology*, vol. 264, pp. 113–132, 2002.
[47] R. H. Hawkins, T. J. Ward, D. E. Woodward, and J. A. Van Mullem, "Curve number hydrology: State of the practice," *American Society of Civil Engineers*, 2008.
[48] E. R Sardoii, N. Rostami, S. K. Sigaroudi, and S. Taheri, "Calibration of loss estimation methods in HEC–HMS for simulation of surface runoff (Case Study: Amirkabir Dam Watershed, Iran)," *Adv. Environ. Biol*, vol. 6, no. 1, pp. 343–348, 2012.
[49] K. H. Zou, K. Tuncali, and S. G. Silverman, "Correlation and simple linear regression," *Radiology*, vol. 227, no. 3, pp. 617–628, 2003.
[50] D. N. Moriasi, J. G. ArnoldVan, M. W. Liew, R. L. Bingner, R. D. Harmel, and T. L. Veith, "Model evaluation guidelines for systematic quantification of accuracy in watershed simulations," *Transactions of the ASABE*, vol. 50, no. 3, pp. 885–900, 2007.
[51] A., Bárdossy and G. Pegram, "Combination of radar and daily precipitation data to estimate meaningful sub–daily point precipitation extremes," *Journal of Hydrology*, vol. 544, pp. 397–406, 2017.
[52] J. L. McKee and A. D. Binns, "A review of gauge–radar merging methods for quantitative precipitation estimation in hydrology," *Canadian Water Resources Journal/Revue canadienne des ressources hydriques*, vol. 41, no. 1–2, pp. 186–203, 2016.
[53] S. I. Ahmed, R. Rudra, P. Goel, A. Khan, B. Gharabaghi, and R. Sharma, "A comparative evaluation of using rain gauge and NEXRAD radar–estimated rainfall data for simulating streamflow," *Hydrology*, vol. 9, no. 8, p. 133, 2022.